PMFSEL 93-6
NOVEMBER 1993

LIMIT STATE PERFORMANCE OF HIGH STRENGTH REINFORCED CONCRETE COLUMNS

By

Rodney Jay Pharis
Richard W. Furlong

with support from
National Science Foundation
Grant No. MSS-9017042

Any opinions, findings, conclusions, or recommendations expressed in this publication are those of the author and do not necessarily reflect the views of the National Science Foundation.

ABSTRACT

ACKNOWLEDGEMENTS

TABLE OF CONTENTS

LIST OF FIGURES

LIST OF TABLES

CHAPTER 1
INTRODUCTION

1.1 Background

Normally, new materials are not used in structural design until extensive research has been conducted to evaluate the performance of these materials. However, structures are currently being built with design concrete strengths of up to 18 ksi (Randall 1989), which is over twice the values from which 40 years of experience and research have led to the recommendations in the ACI Building Code (ACI 318 1989). This has created an urgent need for experimental work in the area of high strength concrete.

Previous and current studies involving high strength concrete have dealt primarily with the following topics:

- Properties of plain high strength concrete (Carrasquillo 1981, Cook 1989, ACI Committee 363 1984).
- High strength reinforced concrete in flexure (Leslie 1976).
- Compression of high strength reinforced concrete confined by lateral reinforcement (Fafitas 1985, Kaar 1978).

Limited experimental work on conventionally reinforced high strength concrete in compression has been conducted.

The purpose of this research project was to evaluate the behavior of high strength reinforced concrete columns with conventional reinforcement. In other words, the spacing of transverse reinforcement was near the maximum allowed by the ACI Building Code, and no significant confinement was provided.

1.2 Scope

1.2.1 Testing. The experimental phase of the project consisted of testing 15 column specimens to failure. Load was applied at relatively low eccentricities so that the entire column cross-section remained in compression. Of the 15 specimens, 10 were cast of high strength concrete while the other 5 were normal strength concrete specimens. The normal strength specimens were used mainly for comparison purposes.

In order to investigate the post-yield buckling tendencies of the longitudinal reinforcement, both the tie spacings and longitudinal reinforcement strength were varied. Using grade 150 steel eliminated prior yielding of the longitudinal reinforcement allowing for determination of the maximum steel stress before concrete crushing. Tie spacings smaller than those required by the current ACI Code were intended to stabilize longitudinal reinforcement and prevent cover concrete from prematurely spalling.

1.2.2 Analysis. In the analysis phase of this project, methods of computing the ultimate capacity of the high strength specimens were investigated. Current design practice using a rectangular

concrete stress block was evaluated based on its accuracy and appropriateness with regard to the behavior of high strength concrete. Then, based on the same criteria, the implementation of a triangular stress block was investigated.

1.3 Overview

The remainder of this report consists of discussion and evaluation of the following topics:

- **Testing Program** (Chapter 2): scope of the tests, specimen descriptions including concrete mix proportions and steel properties, test set-up, measurements and instrumentation, and testing procedures.

- **Test Results** (Chapter 3): stress-strain characteristics of plain high strength concrete, and overall behavior of the column specimens including measurements taken near failure.

- **Analysis and Discussion of Results** (Chapter 4): evaluation of analytical procedures and effects of test variables.

- **Conclusions** (Chapter 5): summary of results and analysis.

CHAPTER 2
TESTING PROGRAM

2.1 Overview

All of the testing and construction was performed at Ferguson Structural Engineering Laboratory of The University of Texas at Austin. The purpose of the tests was to determine the limiting strengths and strains of reinforced concrete columns made of high strength materials and loaded at low eccentricities.

In this chapter, the scope of the testing program is discussed. Then, a description is given of the following topics: specimen descriptions, loading configuration, measurements and instrumentation, preparation for testing, and testing procedure.

2.2 Scope of the Testing Program

In all, fifteen specimens were tested to failure. Ten specimens were made with high strength concrete, and the remaining five specimens were cast with normal strength concrete. Other variables within the scope of this project include the following:

- Strength of the longitudinal steel.
- Arrangement of the longitudinal steel.
- Spacing of the transverse reinforcement.
- Amount of applied eccentricity in loading.

Of the fifteen specimens, eight were prototype specimens and the remaining seven were model specimens. For the prototype specimens a clear cover of 1.5 in. and #3 ties were used in accordance with the ACI Building Code (ACI 318 1989). The model specimens were a 40% scale model of a 20 in. by 20 in. cross section. Consequently, the cover was reduced to 5/8 in. and W2.5 deformed wire was used for transverse reinforcement.

2.3 Specimen Descriptions

2.3.1 Size. All of the specimens were intended to have identical size and shape as shown in Figure 2.1. Each specimen had a total length of 76 in.; however, only the middle 40 in. constituted the actual test region. The tapered end sections were used in order to distribute the load uniformly and prevent localized failure in these end regions. The central test region was 8 in. by 8 in. square in cross-section.

2.3.2 Concrete Properties.

2.3.2.1 Mix Design. A combination of fly ash, silica fume, and superplasticizer was used along with the normal constituents of portland cement concrete to obtain a concrete mix with the desired high strength and high slump. Type II cement was used with relatively large amounts of Class C fly ash and silica fume. The amount of fly ash was about 50% by weight of the cement while the amount of silica

fume was about 11% of the combined weight of cement and fly ash. Rheobuild 1000 superplasticizer was added both at the concrete plant and at the casting site in order to obtain the 8 in. slump necessary for placement. Table 2.1 shows representative proportions of both the high strength and normal strength mixes.

Crushed limestone from Burnet, Texas was used for the coarse aggregate. In order to maintain model similitude, the concrete in all mixes was modelled with aggregates scaled to 40% size (Breen 1970). This model similitude resulted in a nominal maximum size aggregate of 3/8 in.

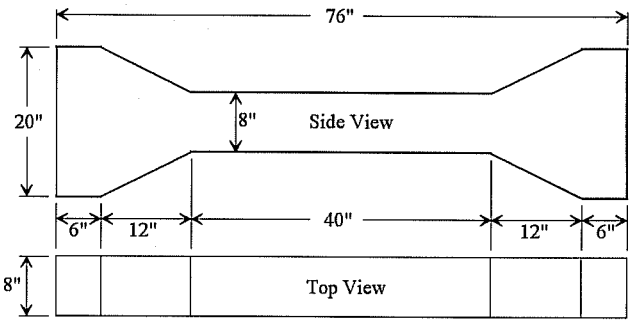

Figure 2.1 Specimen dimensions

2.3.2.2 Curing. Both the column specimens and the concrete cylinders were moist cured for a minimum of 14 days. Column specimens were covered with plastic while they remained in the wood forms. The forms were removed 3 days after casting. Then, the specimens were covered with moist burlap for the remainder of moist curing. Concrete cylinders were covered with moist burlap for the duration of the curing period.

2.3.2.3 Strength. Concrete strengths of 14,000 psi and 6000 psi were targeted. Four concrete pours were required to cast the ten high strength columns, while only two casting dates were required for the five normal strength concrete columns. Compressive strengths obtained from the testing of 6 in. by 12 in. cylinders on specimen testing dates ranged from 5070 psi to 6330 psi for the normal strength concrete, and from 13,040 psi to 16,830 psi for the high strength concrete.

2.3.2.4 Stress-Strain Properties. Stress-strain data was also obtained from the cylinder compression tests. Cylinders from each of three high strength concrete mixes and two normal strength concrete mixes were tested with electrical strain gages that were epoxied to the cylinders. Longitudinal as well as transverse strain gages were placed on opposing sides of each cylinder. The use of a data

Table 2.1 Concrete mix proportions per yd^3

	14,000 psi Concrete	6000 psi Concrete
Cement (lb)	581	562
Class C Fly Ash (lb)	312	0
Silica Fume (lb)	100	0
Water (lb)	278	280
Coarse Aggregate (lb)	1943	1625
Fine Aggregate (lb)	1188	1475
Superplasticizer (oz.)	290	20

acquisition system made it possible to take strain readings while loading at a rate within the ASTM limits (ref). Results of these cylinder tests are presented in chapter 3.

2.3.3 Longitudinal Reinforcement.

2.3.3.1 Type. Longitudinal reinforcement was either grade 60 or grade 150 steel. Specimens consisted of one of the following combinations of concrete and reinforcing bars:

- High strength concrete and grade 60 steel.
- High strength concrete and grade 150 steel.
- Normal strength concrete and grade 150 steel.

Either #4 or #7 bars were used for grade 60 longitudinal reinforcement. All grade 150 reinforcement consisted of #5 Diwidag bars.

2.3.3.2 Arrangement. The arrangement of longitudinal reinforcement varied, depending on whether the specimen was a prototype or a model. All of the bars were uniformly spaced with prototype specimens having a design clear cover of 1.5 in., and model specimens having a design clear cover of 5/8 in. The different arrangements for prototype specimens include the following:

- High strength concrete and 4 #7 bars (Figure 2.2a).
- High strength or normal strength concrete and 8 #5 Diwidag bars (Figure 2.2b).

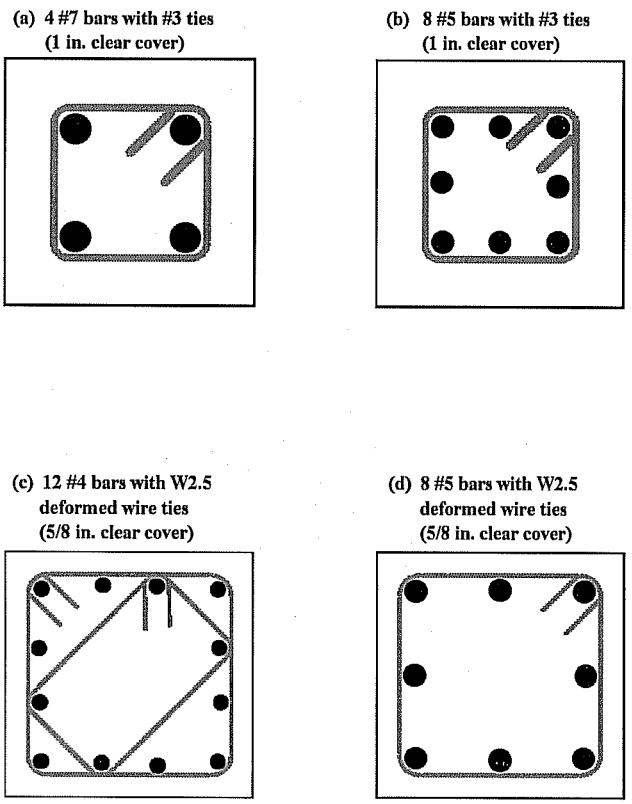

Figure 2.2

Two additional bar arrangements were used for the model specimens:

- High strength concrete and 12 #4 bars (Figure 2.2c).
- High strength or normal strength concrete and 8 #5 Diwidag bars (Figure 2.2d).

2.3.3.3 Strength Properties. Tensile tests were performed on the reinforcement using an 8 in. linear extensiometer to measure the steel strain. Stresses and strains were monitored with an X-Y plotter. Each of the bars was tested at a constant strain rate that resulted in yielding in about 5 minutes. This corresponds with the alternate method of testing given by ASTM A370. The lower testing rate was used in order to obtain measurements applicable to reinforcing steel in the column tests.

For all of the grade 60 reinforcement, there was a distinct yield point. Figure 2.3a shows the stress-strain characteristics of the grade 60 bars. An average yield stress of 68 ksi for the

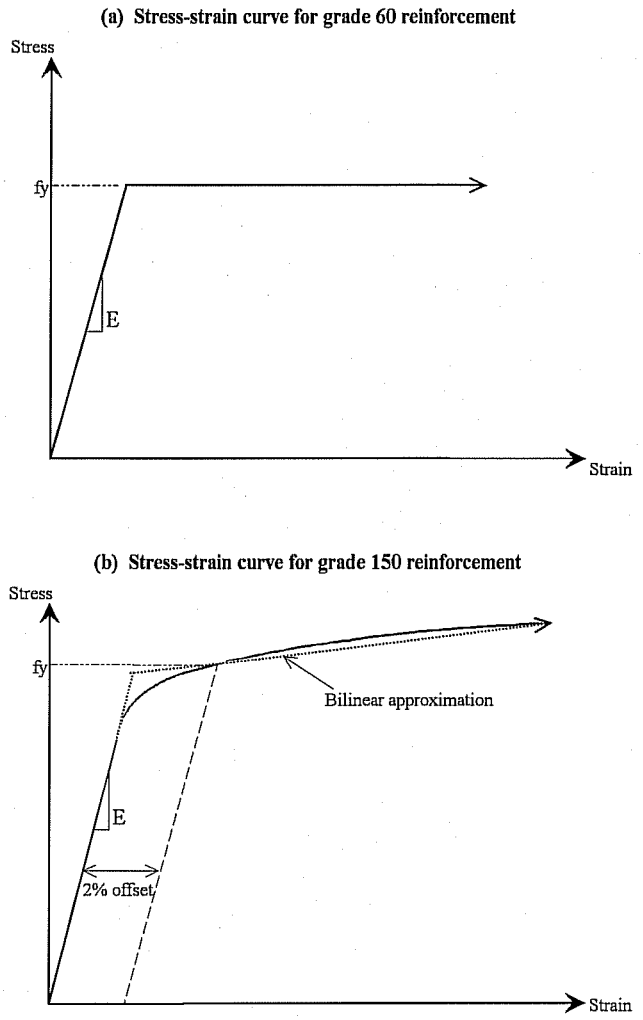

Figure 2.3

#4 bars and 65 ksi for the #7 bars was obtained from testing. Corresponding ultimate steel stresses were 104 ksi for the #4 bars and 103 ksi for the #7 bars.

The grade 150 #5 Diwidag bars had no distinct yield point. As shown by Figure 2.3b, the stress-strain response of the #5 bars was approximately bilinear with a slope in the stain-hardening region of about 1170 ksi. Based on a cross-sectional area of 0.28 in^2, an average yield stress of 131 ksi and an ultimate stress of 161 ksi were computed for the Diwidag bars. From weight measurements, the area of a #5 Diwidag bar was determined to be 0.28 in^2. This bar area rather than the nominal 0.31 in^2 was used for stress calculations since the German made Diwidag bar has slightly different dimensions than a reinforcing bar made in the United States.

2.3.4 Transverse Reinforcement. Rectangular ties with 135 degree bends were used for transverse reinforcement. The 135 degree hooks were never placed in the compression face of the eccentrically loaded columns. Also, the hooks were alternated from side to side.

Transverse reinforcement for the prototype specimens was restricted to #3 ties with an average ultimate strength of 72 ksi. Spacing of these ties varied from 5 in. to 8 in. For each of the prototype specimens, the longitudinal bars were enclosed by single rectangular ties as shown in Figures 2.2a and 2.2b.

W2.5 deformed wire with an average ultimate strength of 99 ksi was used for all of the model specimens. Spacing of the deformed wire ties also ranged from 5 in. to 8 in. Model specimens with 8 #5 longitudinal bars were enclosed by single rectangular ties as shown by Figure 2.2d. However, an arrangement using two rectangular ties as shown in Figure 2.2c was implemented for the model specimens which contained 12 #4 longitudinal bars.

The end regions outside the central 40 in. length were heavily reinforced to prevent failure in those regions. #4 ties at 2.5 in. spacing were used for the high strength concrete specimens, and #3 ties at 2.5 in. spacing were used for the normal strength concrete specimens.

2.3.5 Summary of Specimen Parameters. A summary of the various parameters for each specimen is given in Table 2.2. In order to identify each specimen, the following notation was used:

Table 2.2 Summary of specimen parameters

Specimen Number	Specimen Designation	Eccen. of Load (in.)	Concrete f'c (psi)	Longitudinal Reinf.	Transverse Reinf.
1	CPNH1	0.5	6329	8 #5	#3 @ 7.5"
2	CPNH3	1.0	6437	8 #5	#3 @ 7.5"
3	CPHH1	0.5	14064	8 #5	#3 @ 7.5"
4	CPHH3	1.0	14145	8 #5	#3 @ 7.5"
5	CPHN3	1.0	14397	4 #7	#3 @ 8"
6	CPHN1	0.5	14449	4 #7	#3 @ 8"
7	CMHN1	0.5	16635	12 #4	W2.5 @ 8"
8	CMHN2a	0.5	16833	12 #4	W2.5 @ 6"
9	CPHH2	0.5	16150	8 #5	#3 @ 5"
10	CMHN2b	0.5	13195	12 #4	W2.5 @ 6"
11	CMHH1	0.5	13040	8 #5	W2.5 @ 7.5"
12	CMHH2	0.5	13673	8 #5	W2.5 @ 5"
13	CPNH2	0.5	5070	8 #5	#3 @ 5"
14	CMNH1	0.5	5363	8 #5	W2.5 @ 7.5"
15	CMNH2	0.5	5488	8 #5	W2.5 @ 5"

- The first letter, "C", stands for column.
- The second letter indicates whether the specimen is a prototype, "P", or a model, "M".
- The third letter specifies whether the concrete is high strength, "H" or normal strength, "N".
- The fourth letter specifies whether the steel is high strength, "H", or normal strength, "N".
- For the ending number, "1" and "2" are reserved for 0.5 in. eccentricity while "3" indicates that the specimen was loaded at 1.0 in. eccentricity. "1" corresponds to a larger tie spacing than "2".
- Specimens 8 and 10 are identical and are distinguished by an "a" and "b" respectively.

2.3.6 Construction. Each of the fifteen specimens was constructed at Ferguson Laboratory. Either two or three specimens were fabricated at one time. The construction process involved three stages: assembling the forms, constructing the steel cages, and casting the concrete.

Reusable wooden forms were made in four pieces that could be easily bolted together. The forms were waterproofed and sealed before placing the concrete.

The steel cages were constructed taking special care to control the dimensions of each specimen. Complete fabrication of the steel cages was performed in the laboratory including cutting the reinforcing bars to length, bending the transverse reinforcement, and tying the steel in place. Figure 2.4 shows a completed reinforcement cage resting inside one of the wooden forms.

The concrete was obtained from Capitol Aggregates, a local ready-mix plant. Columns were cast vertically so that realistic conditions could be simulated. Three lifts of concrete along with internal vibration were necessary to ensure good consolidation.

Figure 2.4 Completed reinforcement cage

2.4 Loading Configuration

Specimens were tested in a horizontal position. Loads were transmitted from a hydraulic ram to a specimen through a series of steel plates and rollers as shown in Figure 2.5. The end plates were supported from above by either a flexible chain or a rod capable of rotating. Figure 2.6 shows a detail of the rollers at the column ends which allowed the specimen to rotate freely.

Loads were applied eccentrically below the column centroid as shown by Figure 2.7 producing the highest compressive forces on the bottom face. The eccentricity could be changed by simply adjusting the two supports to any desired height. When a flat steel plate was used in place of the rollers for specimens 1 and 2, very unpredictable eccentricities resulted. With the rollers, eccentricity of the applied load could be accurately controlled.

2.5 Measurements and Instrumentation

2.5.1 General Scheme. A complete set of data was essential in attempting to understand the behavior of each specimen. As a result, it was thought necessary to take the following measurements:

- Specimen dimensions and gage locations.
- Axial load.
- Exterior concrete strains.
- Deflections and end rotations.

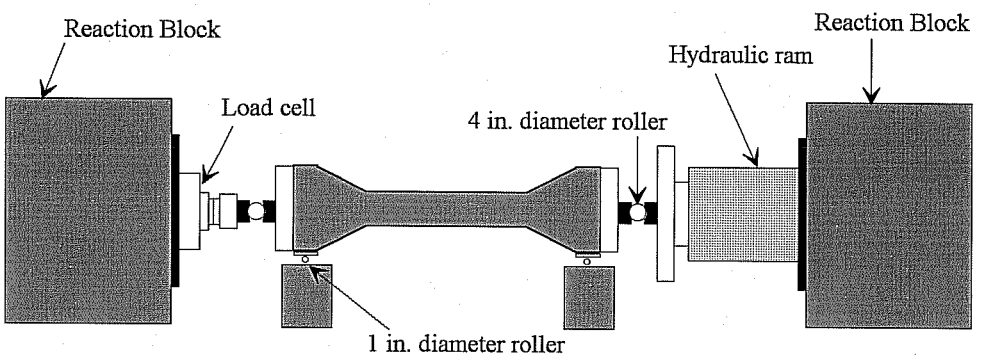

Figure 2.5 Test set-up

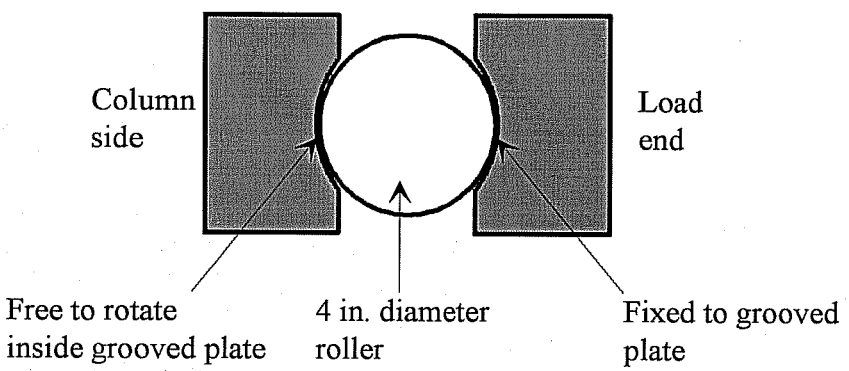

Figure 2.6 Detail of end roller

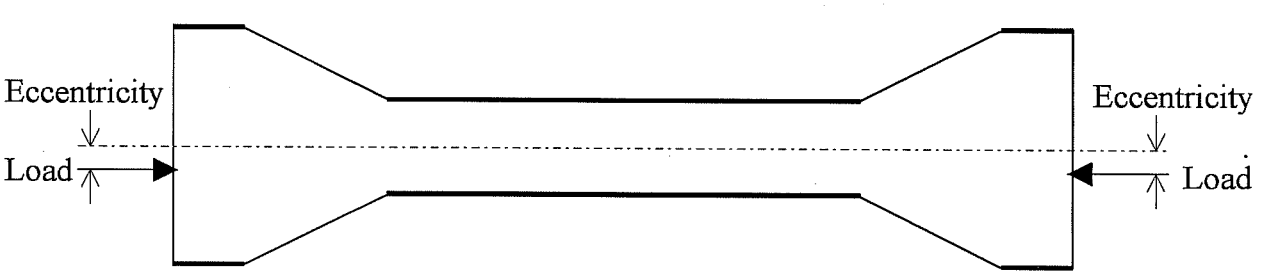

Figure 2.7 Diagram showing loading eccentricity

Due to a large amount of instrumentation, a data acquisition system was used to expedite the testing process and to facilitate data reduction..

2.5.2 Specimen Dimensions and Gage Locations. In general, there was some variability, but the overall dimensions and gage locations were approximately the same for each specimen. An effort to place gages in areas with minimal defects resulted in a difference in gage locations, and the dimensions of each specimen were slightly different depending on the form used. Consequently, the actual position of the gages and the cross-sectional dimensions were measured for every column. In addition, longitudinal bar locations were measured for bars exposed at each end after casting the concrete.

2.5.3 Axial Load Measurements. A load cell at the north end of the test set-up was the primary source for measuring axial load. A hydraulic pressure transducer served as a secondary measure for force on the loading ram.

2.5.4 Exterior Concrete Strains. Longitudinal strains as well as transverse strains were measured with 2 in. electrical strain gages. These strain gages were placed on the column faces at three cross-sections along the testing region. The cross-sections were located at midlength and 10 in. on either side of midlength.

As a back-up to verify strain gage readings, mechanical gage points known as DEMEC points were attached with epoxy at 8 in. intervals along the east and west sides of the specimens. A DEMEC point is a small stainless steel disk with a tiny hole in the center for inserting the DEMEC gage. The DEMEC gage measures the distance between two points so that an average strain over the 8 in. gage length can be obtained from a change in gage readings. In previous work at Ferguson Laboratory, this system of measurement has proven to be reliable and accurate to within 20 or 30 microstrains (Castrodale 1988).

Normally, 24 strain gages and 16 DEMEC points were used for each specimen. Figure 2.8 shows the approximate locations of these gages. For specimens 1 and 2, neither gages 9, 12, 13, and 16 nor the DEMEC points were included.

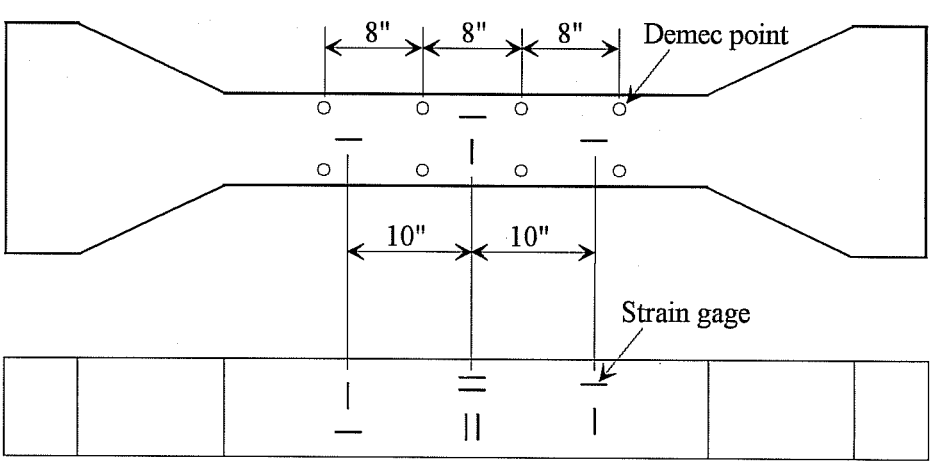

Figure 2.8 Strain gage and Demec point locations

2.5.5 Deflections and End Rotations. In order to further monitor the behavior of each column, it was necessary to measure deflections and end rotations. Linear potentiometers were the primary device for measuring deflections while mechanical dial gages were used as a secondary device. Two microlevels, one at each end bearing plate, provided for rotation data.

Figure 2.9 shows the locations of the linear potentiometers, dial gages and microlevels. Five linear pots along with three dial gages were placed along the top face at 10 in. intervals to measure vertical deflections. A single linear pot at midlength of the east face was used to monitor any horizontal movement. Also, north-south translation was measured with four linear pots located at the ends of the east and west faces.. The microlevels were clamped to the end bearing plates of each specimen.

2.5.6 Data Acquisition. Since much of the instrumentation was electrical, the use of a data acquisition system was very advantageous. Readings from the electrical gages including the load cell, pressure transducer, strain gages, and linear potentiometers could be taken almost instantaneously. This tremendous savings in time was further amplified by the fact that all of the recorded data could be directly transferred to a spreadsheet for data reduction. Also, the data acquisition system kept to a minimum any recording errors.

A further benefit of the data acquisition system was that readings of load and strain could be taken all the way to failure. Since the specimen failures were extremely violent, the mechanical gages were recorded only up to about 70% of the estimated failure load, after which the mechanical gages were removed and protective shielding was placed around the specimen.

2.6 Preparation for Testing.

In preparing to test, special care was taken properly to align the column so that a constant eccentricity of known magnitude could be applied and biaxial bending could be kept to a minimum. After alignment, a thin layer of hydrostone was poured in between the column ends and the adjacent steel plate. This ensured a smooth loading surface perpendicular to the axis of the column.

Before testing, an anti-seize compound was applied to the rollers. Also, a check was performed to make sure all of the instrumentation was functioning properly.

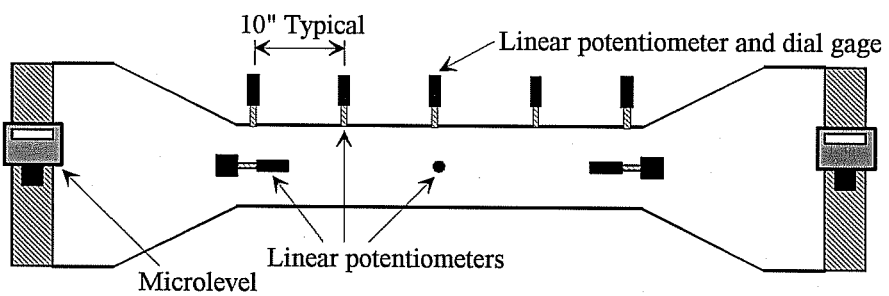

Figure 2.9 Typical locations of dial gages, linear potentiometers, and microlevels

2.7 Testing Procedure.

The actual testing of the specimen from zero load to failure lasted approximately 2 hours. Since 15 to 20 load increments were desired, the high strength concrete specimens were loaded in 50 kip increments while the normal strength concrete specimens were loaded in 25 kip increments.

At low loads, the DEMEC gage lengths, dial gages, and microlevels were manually read and recorded, and the electrical readings were taken with the data acquisition system for each loading increment. Before any loads were increased, a "creep" reading was taken of each gage; however, "creep" readings were not taken of the DEMEC gage lengths. The time between the initial load reading and the creep reading was typically about 6 to 8 minutes.

When the load reached about 70% of the estimated failure load, certain safety precautions had to be taken. The dial gages, linear potentiometers, and microlevels were removed from the test set-up to prevent them from being damaged. In addition, sheets of plywood were placed on both sides of the specimen to protect the researchers from flying debris at failure.

For the remainder of the test, only the loads and strain readings could be monitored. Two readings, one immediately after the load was applied and a creep reading about 3 minutes later, were taken at each load increment. When the creep strains became significantly large, the increment of load was reduced in half. Loading proceeded in this manner until the specimen failed.

CHAPTER 3
TEST RESULTS

3.1 Scope of the Test Results

A major concern during the testing process was to obtain reliable data so that an accurate analysis of the specimens could be performed. Pertinent stress-strain information for the concrete was acquired from cylinder compression tests. During the testing of column specimens, important data taken included measurements of loads, strains, deflections, and end rotations.

3.2 Overview

In this chapter, the stress-strain characteristics of high strength concrete cylinders are evaluated. Then, the overall behavior of the column specimens including observations made and measurements taken throughout testing is examined and discussed. Lastly, the behavior of the columns are compared with the behavior of the cylinders.

3.3 Concrete Stress-Strain Characteristics

3.3.1 Results from Cylinder Compression Tests. As previously described, cylinders with electrical strain gages affixed to the sides were tested in compression to obtain the stress-strain characteristics of the concrete used for casting the column specimens.

Because of the extremely brittle nature of the high strength concrete, it was not possible to obtain any of the downward portion of the stress-strain curves after the peak stress was reached. The failures of the high strength concrete cylinders were very sudden and explosive as opposed to failures of normal strength concrete cylinders. Beyond the ultimate load, nearly all of the high strength cylinders were completely destroyed while the normal strength concrete cylinders remained mostly intact.

The stress-strain data from the 12 high strength cylinders that were tested is shown in Figure 3.1. For all three high strength mixes, the stress-strain response was approximately linear throughout loading. Consequently, the ultimate strain may be somewhat dependent on the modulus of elasticity of the concrete. A higher modulus of elasticity normally corresponded with a lower ultimate strain.

As shown by Figure 3.2, the behavior of the normal strength concrete cylinders near ultimate load indicates some ductility. Although the downward portion of the stress-strain curve was not obtained, it is apparent that the relationship between stress and strain was nonlinear at relatively high stresses.

3.3.2 Comparing Test Results with the Literature. ACI Committee 363 reports that the ACI 318 equation overestimates the modulus of elasticity for high strength concrete (ACI Committee 363 1984). An alternate equation developed by Nilson is recommended for predicting the modulus of elasticity of high strength concrete. However, higher values of modulus of elasticity have been reported by others. Cook reported that both the ACI 318 equation and the Nilson equation underestimated the

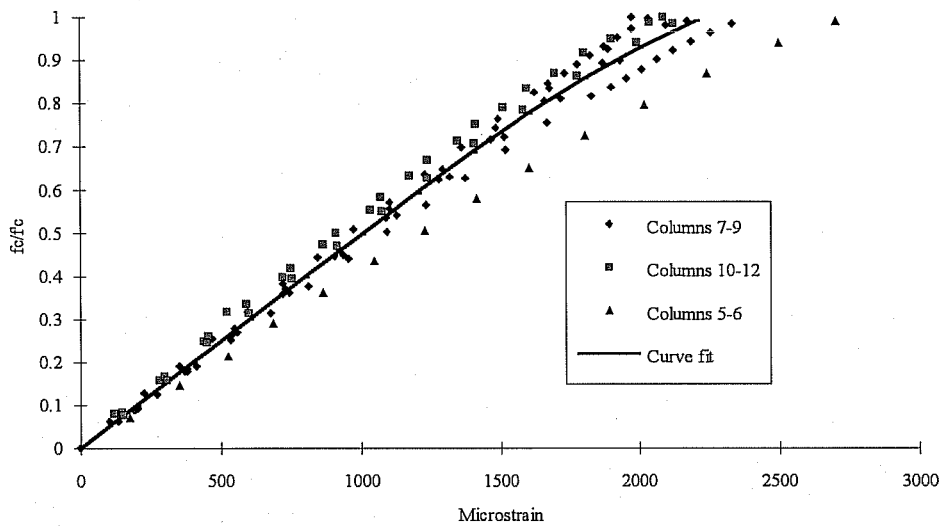

Figure 3.1 Stress vs. strain for high strength concrete cylinders

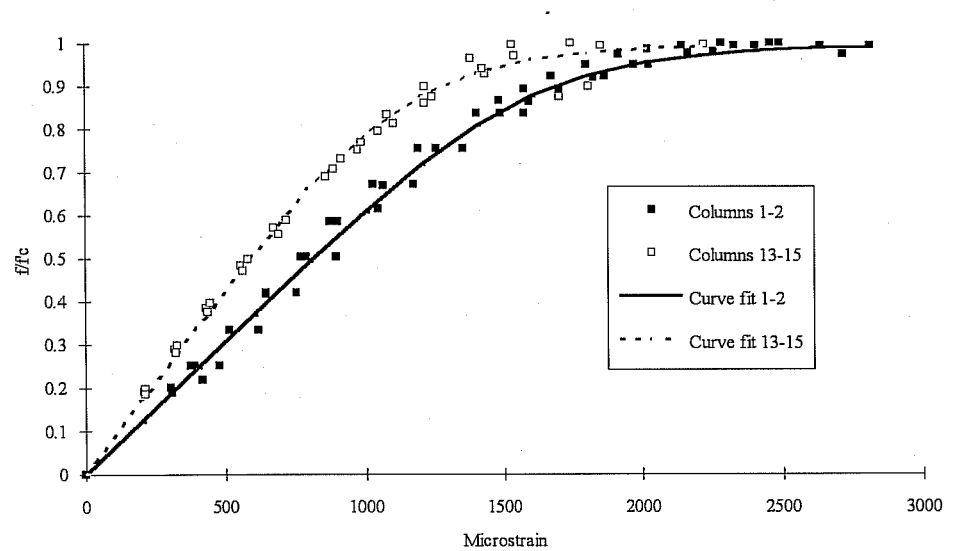

Figure 3.2 Stress vs. strain for normal strength concrete cylinders

measured values of modulus of elasticity for high strength concrete containing aggregates obtained from South Carolina, Tennessee, Texas, and Arizona (Cook 1989). These aggregates included crushed limestones, granites, and native gravels.

As shown in Table 3.1, the modulus of elasticity of 2 of 3 high strength concrete mixes from this experiment correlate very well with the equations of the current ACI Building Code (ACI 318 1989), but the other mix had a modulus of elasticity approximately equal to that predicted by the Nilson equation (ACI Committee 363 1984). This difference in stiffness is attributed to the fact that 8% less coarse aggregate was used in concrete mix 3 than the other high strength concrete mixes.

Table 3.1 Measured vs. predicted modulus of elasticity (E)

Concrete Mix	f'c (psi)	Density (pcf)	Measured E (ksi)	ACI 318 E (ksi)	Nilson E (ksi)
1	6300	144	3860	4530	N.A.
3	14600	148	6070	7180	6010
4	17200	158	8500	8590	7100
5	12900	154	7020	7160	6070
6	5500	144	4630	4230	N.A.

The stiffness of concrete is primarily influenced by the amount and type of coarse aggregate while strength is controlled by the mortar (Carrasquillo 1981). Therefore, if high strength concrete is manufactured by only improving the mortar characteristics, the strength will increase without a proportionate increase in stiffness. However, if the amount of coarse aggregate is increased as well, the stiffness may very well increase proportionally with strength.

Carrasquillo also reported that the stress-strain curve of high strength concrete is more linear up to the maximum stress, and that the descending branch of the stress-strain curve is approximately vertical (Carrasquillo 1981). A typical stress-strain curve for high strength concrete as opposed to normal strength concrete is shown in Figure 3.3. It is apparent that beyond the strain at maximum stress for high strength concrete, no further strain capacity can be relied upon as it can with normal strength concrete. As a result, a reduction in limit strain should be considered for ultimate strength design.

3.4 Learning from Laboratory Experience

Much was learned throughout construction and testing of the column specimens. Using flat plates as end supports resulted in a large amount of biaxial bending for specimens 1 and 2, both of which were constructed of normal strength concrete. Since biaxial bending was not included in the scope of this project, both specimens were not included in any further discussion. Also, specimen 8 was eliminated

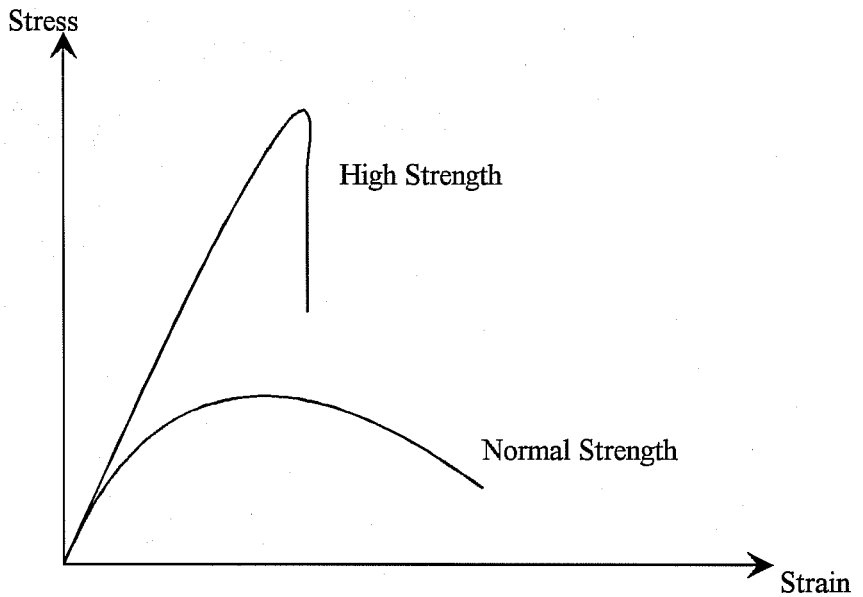

Figure 3.3 Typical stress-strain curve of normal and high strength concrete

from discussion because poor vibration during casting resulted in large sections that had to be repaired. However, both the reinforcement and applied eccentricity were duplicated in specimen 10.

3.5 Overall Behavior of Column Specimens

3.5.1 Load-Strain Relationship. Figure 3.4 displays graphs of load versus average strain at the bottom face or maximum compression face of column specimens. As shown by Figure 3.4, the high strength concrete columns that were tested exhibited very linear behavior even at loads near ultimate. The strain readings shown are an average of the two longitudinal strain gages located on the bottom compression face near the center of each column. Corresponding loads are simply the total axial load on the column.

In contrast to the behavior of the high strength concrete columns, that of the normal strength concrete specimens is significantly nonlinear at high loads. Figure 3.5, shows the load-strain relationship for two of the normal strength concrete columns. The stress-strain results of the cylinder tests were indicative of the load-strain characteristics of the columns.

3.5.2 Correlation of Strains and Deflections with Eccentricity. In order to evaluate the total amount of applied moment including secondary effects, it was necessary to determine the maximum eccentricity for each stage of load. This maximum eccentricity, which normally occurred at midspan, includes the initial eccentricity applied at the ends and the additional eccentricity due to deflections of the column. Figure 3.6 shows both components of the total eccentricity. Strain profiles, end rotations, and deflection measurements were used to determine the maximum eccentricity.

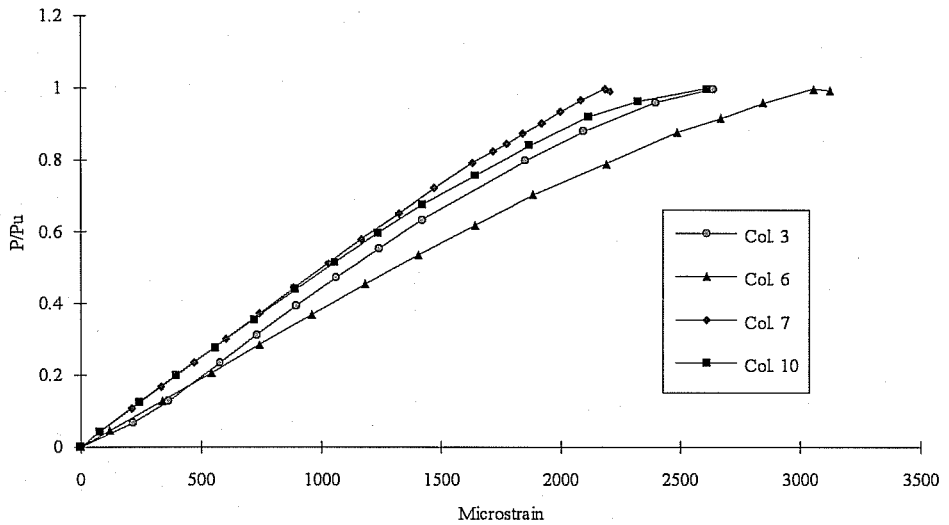

Figure 3.4 Load vs. strain for high strength concrete columns

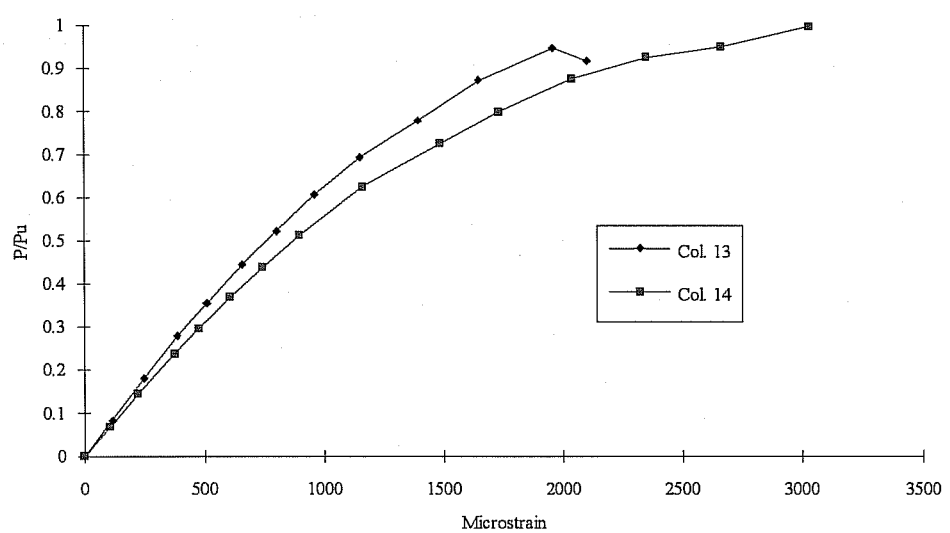

Figure 3.5 Load vs. strain for normal strength concrete columns

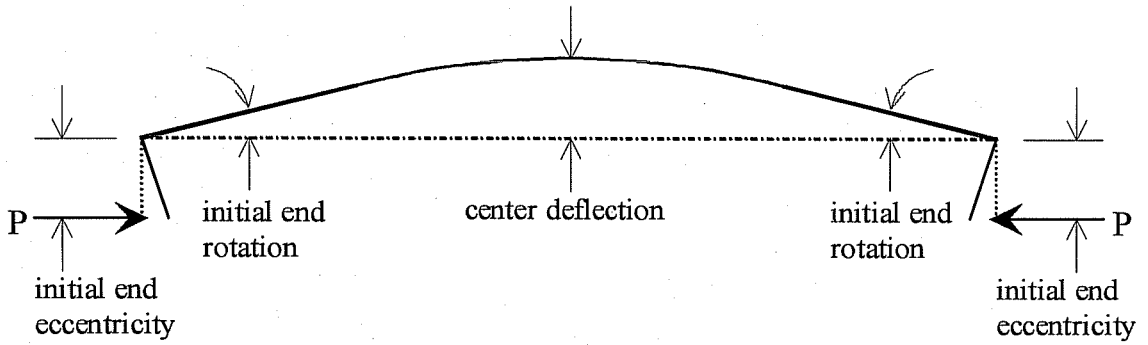

Figure 3.6 The components of eccentricity

3.5.2.1 Strain Profiles. The curvature at a given cross-section could be determined from a strain profile. Figures 3.7a to 3.7d show two strain profiles from a high strength concrete column and two strain profiles from a normal strength concrete column. The assumption that plane sections remain plane seemed to hold true throughout since the strain profiles showed a linear relationship of strain. Also, the DEMEC gage readings were in good agreement with the strain gage readings. These two factors contributed to confidence that was given to the electrical strain gage readings.

3.5.2.2 Deflections. Deflections readings from the linear potentiometers and end rotation readings from the microlevels seemed to be very reliable as well. In most cases, the deflections measured by the linear potentiometers were almost identical to those measured by the mechanical dial gages. Also, the microlevels were consistent with each other. Figures 3.8a to 3.8d show the load-deflection response and the load versus end rotation behavior of specimens 6 and 10.

3.5.2.3 Applied End Eccentricity. The first component of eccentricity, the applied end eccentricity, was known. Careful measurements were taken to locate the centerline of each column and to adjust each end of the column to its desired position. In order to minimize any biaxial bending, the columns were centered horizontally as well.

Curvatures obtained from the electrical strain gage readings were used to verify the initial end eccentricities at low loads. An average curvature of three cross-sections was used for this comparison. For the initial two or three load increments, the eccentricity determined from the measured curvatures differed from the applied eccentricity by about 5 or 10 percent. This difference was attributed mainly to imperfections in the end conditions and in the reinforced concrete column itself. At higher loads, the difference was around 3 percent. The "flaws" in the beginning were not detected at larger loads. Consequently, the initial end eccentricities, either 0.5 in. or 1.0 in., were assumed to be accurate within a few percent.

3.5.2.4 Additional Eccentricity Due to Secondary Effects. Secondary effects were determined from measurements of midspan deflections and end rotations, and strain profiles. The deflection measurements from the linear potentiometers and rotation measurements from the microlevels were considered to be the most reliable sources. Since the linear potentiometers and microlevels had to be removed before the ultimate load was reached, curvatures determined from the strain profiles had to be

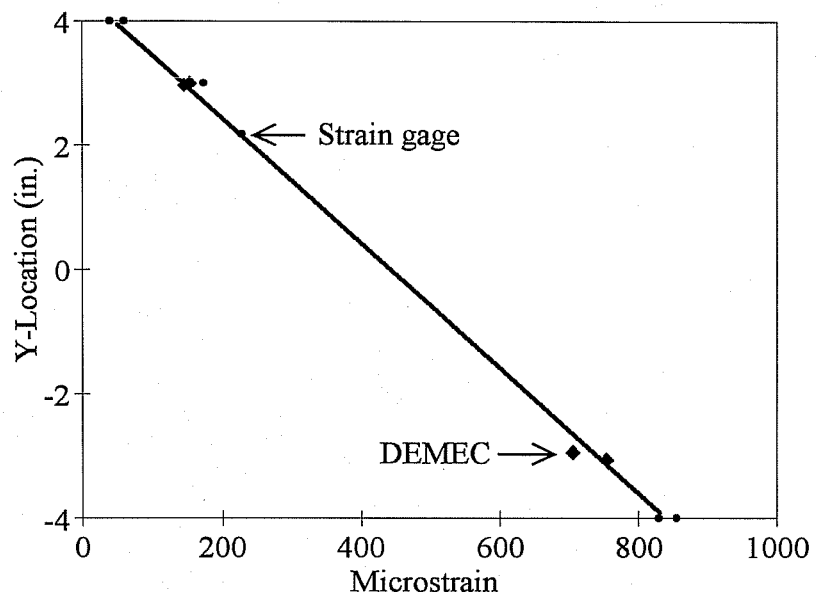

Figure 3.7a Strain profile of specimen 4 at the center cross-section and at a load of 181 kips

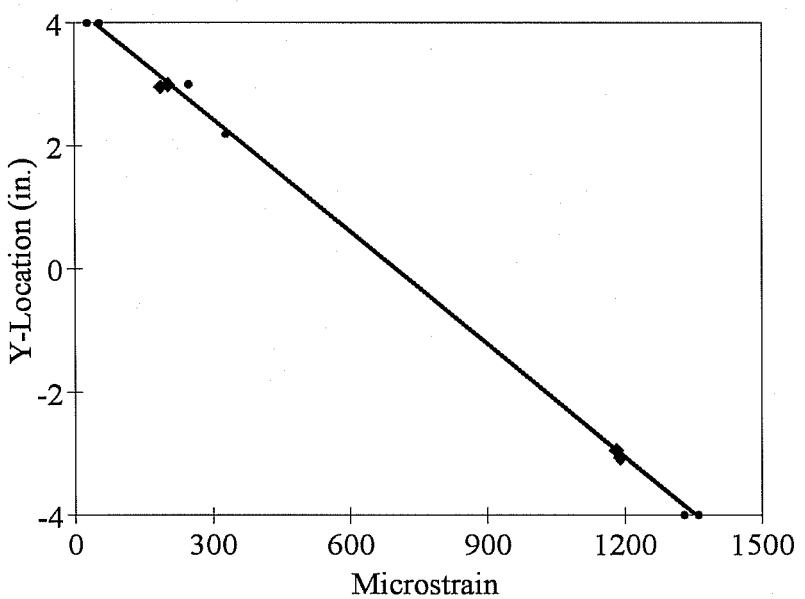

Figure 3.7b Strain profile of specimen 4 at the center cross-section and at a load of 288 kips

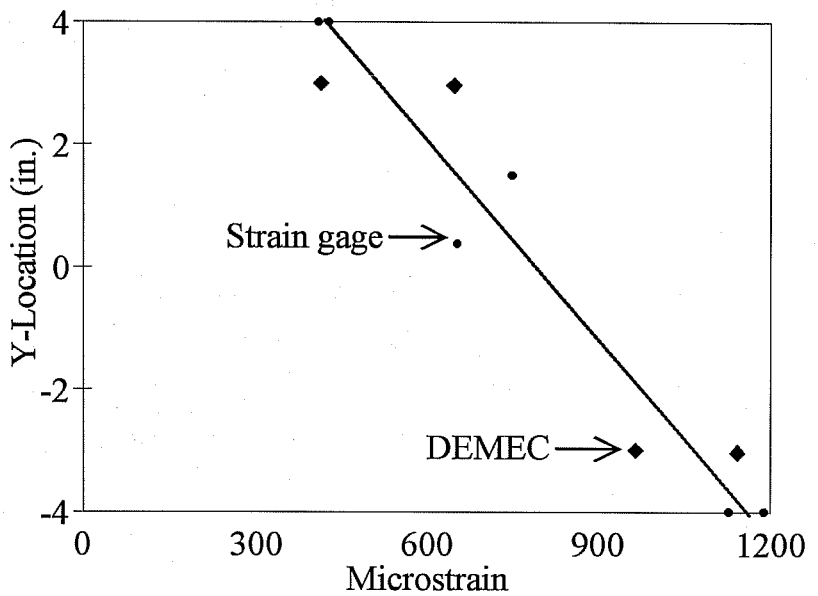

Figure 3.7c Strain profile of specimen 14 at the center cross-section and at a load of 221 kips

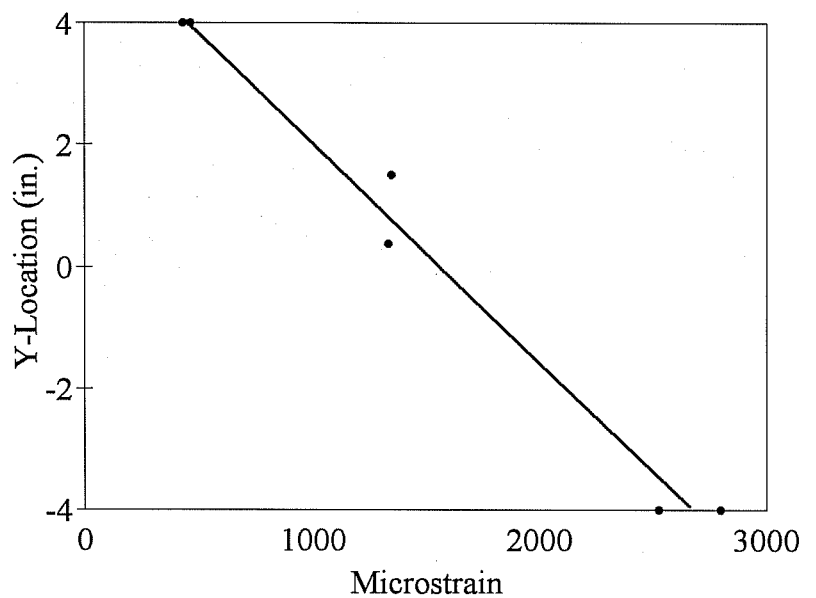

Figure 3.7d Strain profile of specimen 14 at the center cross-section and at a load of 336 kips

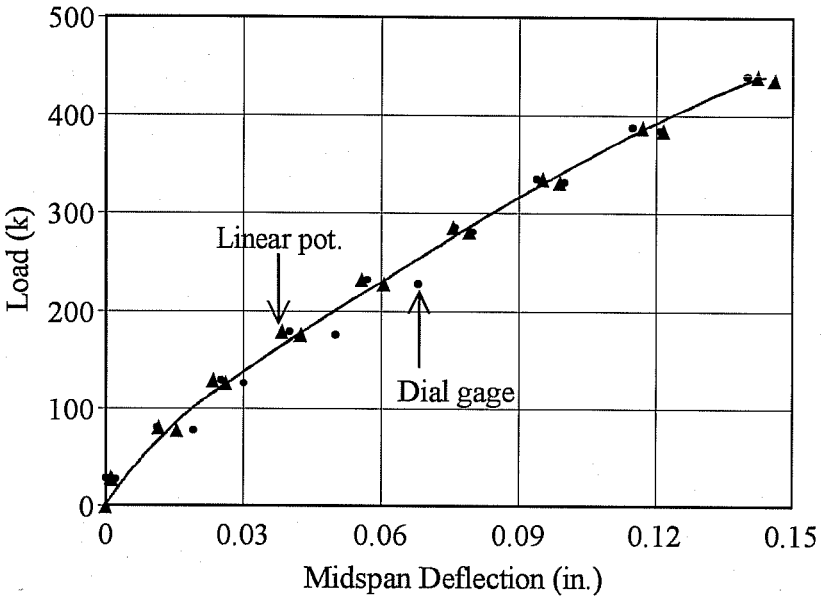

Figure 3.8a Load vs. midspan deflection for specimen 6

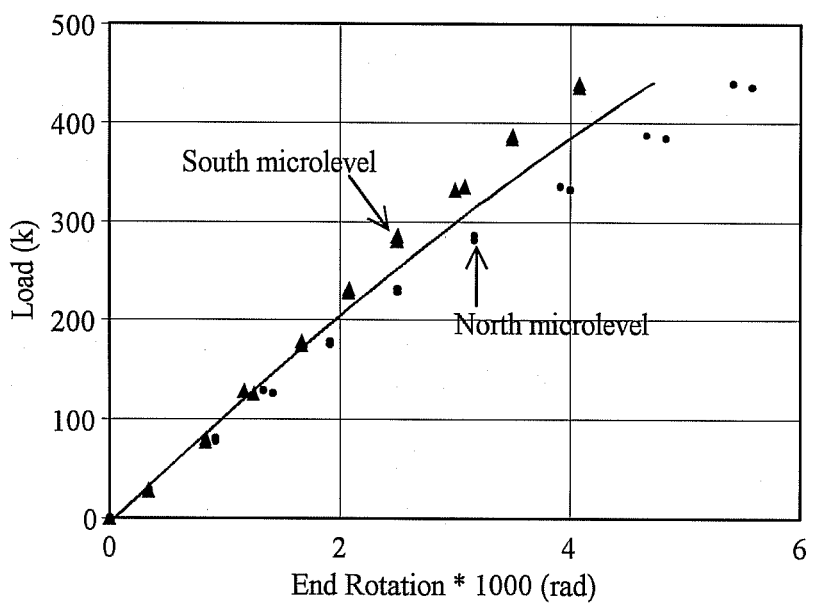

Figure 3.8b Load vs. end rotation for specimen 6

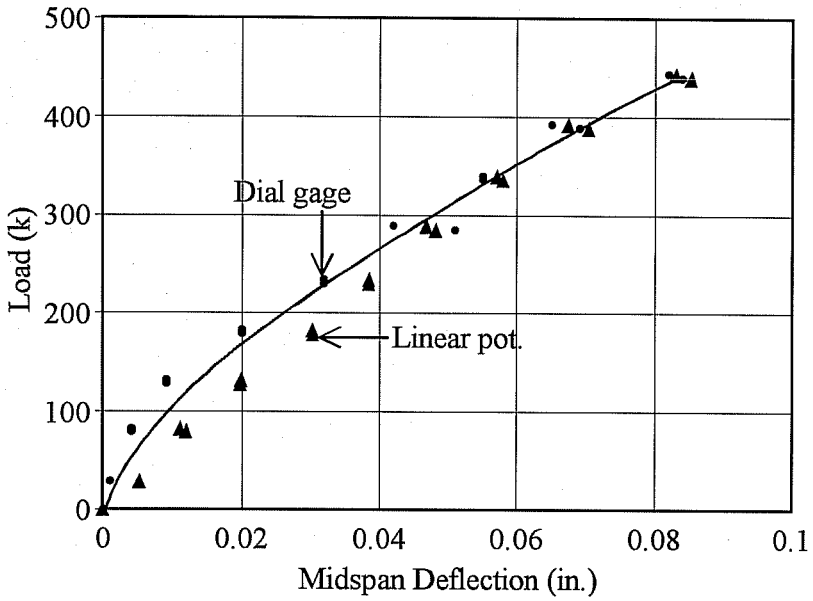

Figure 3.8c Load vs. midspan deflection for specimen 10

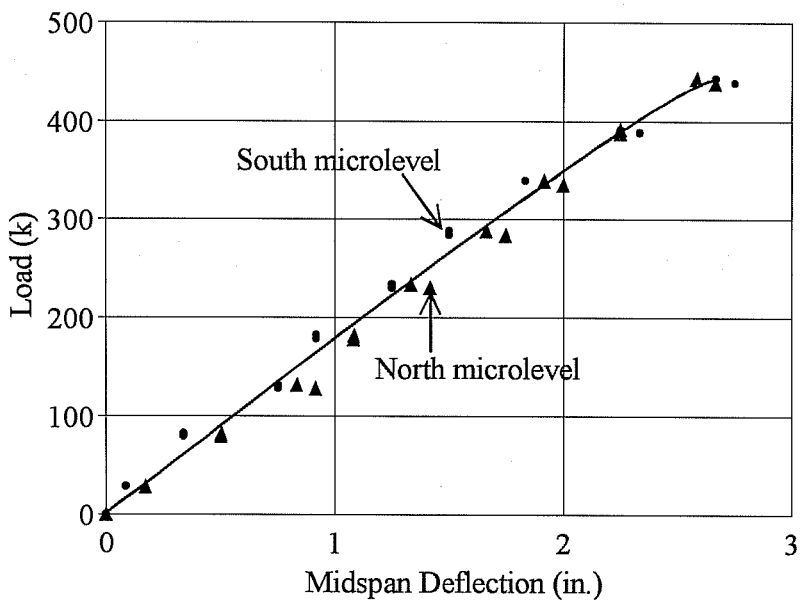

Figure 3.8d Load vs. end rotation for specimen 10

relied on to determine the maximum deflections. For calculating deflections and rotations, a constant curvature equal to the average of the curvatures measured over the 40 in. testing region, was assumed. The effective length over which the average curvatures were applied was determined to be 46 in. by using transformed sections. As shown by Figures 3.9a to 3.9d, the deflections and end rotations calculated from the curvatures compared very well with the measured values.

3.6 Measurements and Observations at Ultimate Load

3.6.1 Description of Specimen Failures. The failures of the high strength reinforced concrete specimens were characteristically explosive and brittle. The first column was pushed into the air beyond the protective plywood (approximately 3 feet). Restraining cables were draped over subsequent specimens to prevent this from recurring. In every high strength concrete specimen failure, pieces of concrete flew as high as 20 feet into the air. Figure 3.10 shows a failed specimen constructed of high strength concrete.

The specimens constructed of normal strength concrete failed in a manner less explosive than the high strength concrete specimens. Figure 3.11 shows a failed normal strength concrete specimen. Before failure, there were definite indications that the normal strength concrete specimens were about to fail. Strains became nonlinear, and there was a significant amount of "creep" strain between loading increments.

From observations made during testing, different mechanisms that could have initiated failure were considered possible. Obviously, the concrete was near its limit capacity when each of the specimens failed, but buckling of the steel reinforcement may have initiated the failure in some cases. For a majority of the specimens, a clicking sound was heard a few seconds prior to failure. Sometimes a second sound of a piece of concrete hitting the ground was heard. This indicated that some of the reinforcing bars may have buckled causing the cover to spall off. For the specimens with grade 60 reinforcement, it is possible that the compression face longitudinal reinforcement may have yielded in compression resulting in its loss of stiffness. Another observation made after failure was that there were broken ties in all of the high strength concrete model columns; however, this may have occurred after the specimen failed.

3.6.2 Measurements at Ultimate Load. Measurements of the maximum axial load, eccentricity, moment, and strain are summarized in Table 3.2. The maximum eccentricity is the total magnified eccentricity, and the maximum moment is the axial load multiplied by the magnified eccentricity. Usually the ultimate axial load could be taken directly from the load cell reading; however, when a specimen failed during loading, the axial load was estimated from the pressure gage which could be read continuously. These measurements were vital in determining the limit state behavior of the column specimens.

3.7 Relating Column Behavior with Cylinder Behavior

The behavior of the columns correlated well with the behavior of the cylinders from a given concrete mix. Table 3.3 indicates the specimens that were cast from each mix.

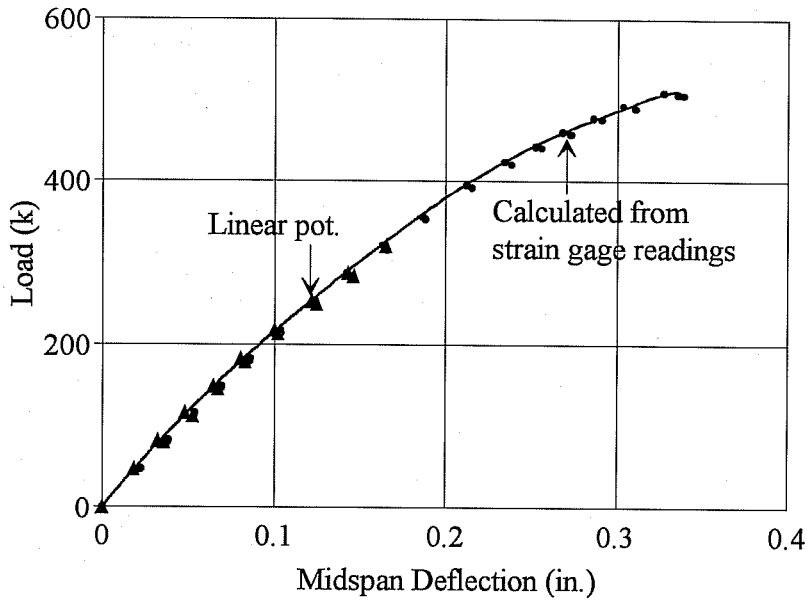

Figure 3.9a Load vs. midspan deflection for specimen 5

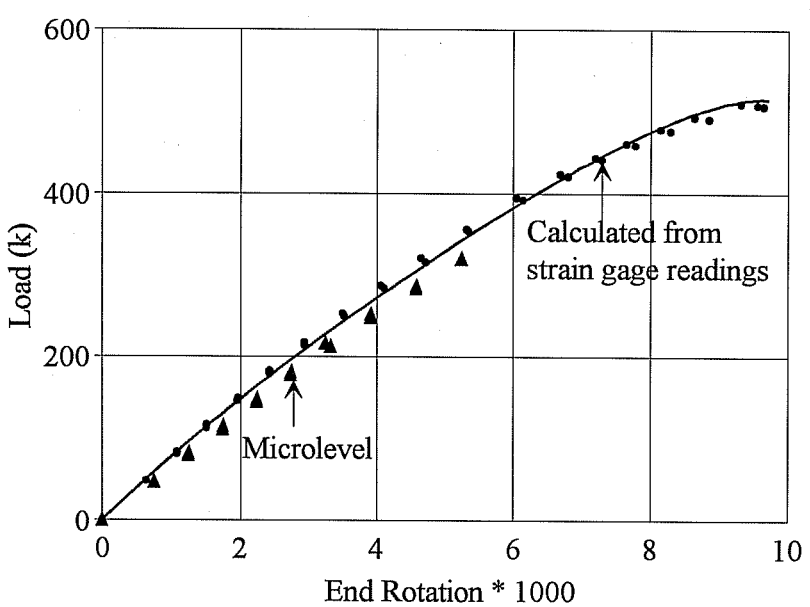

Figure 3.9b Load vs. end rotation for specimen 5

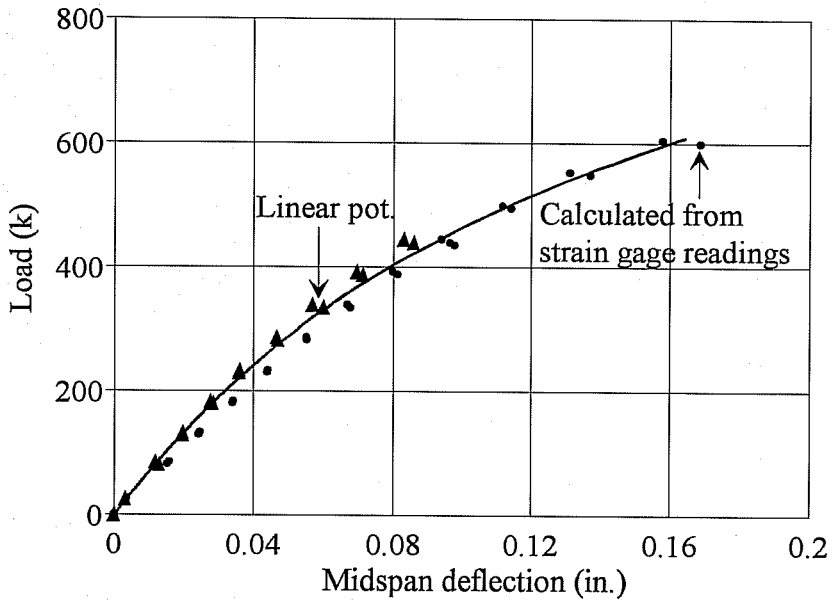

Figure 3.9c Load vs. midspan deflection for specimen 11

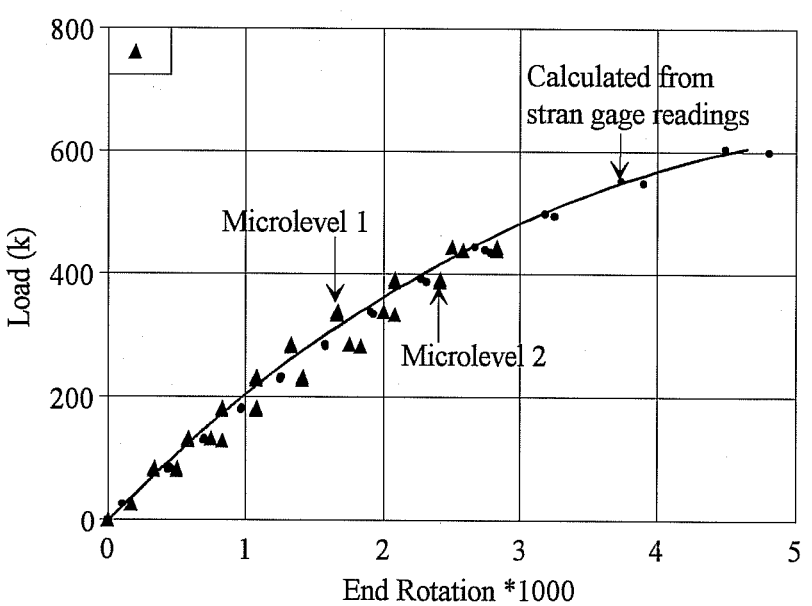

Figure 3.9d Load vs. end rotation for specimen 11

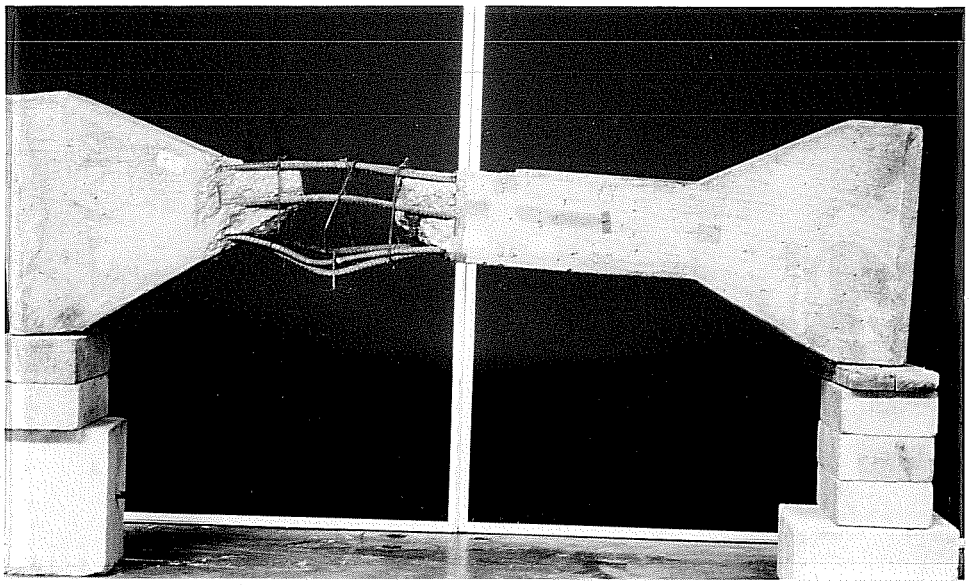

Figure 3.10 Failed high strength concrete specimen

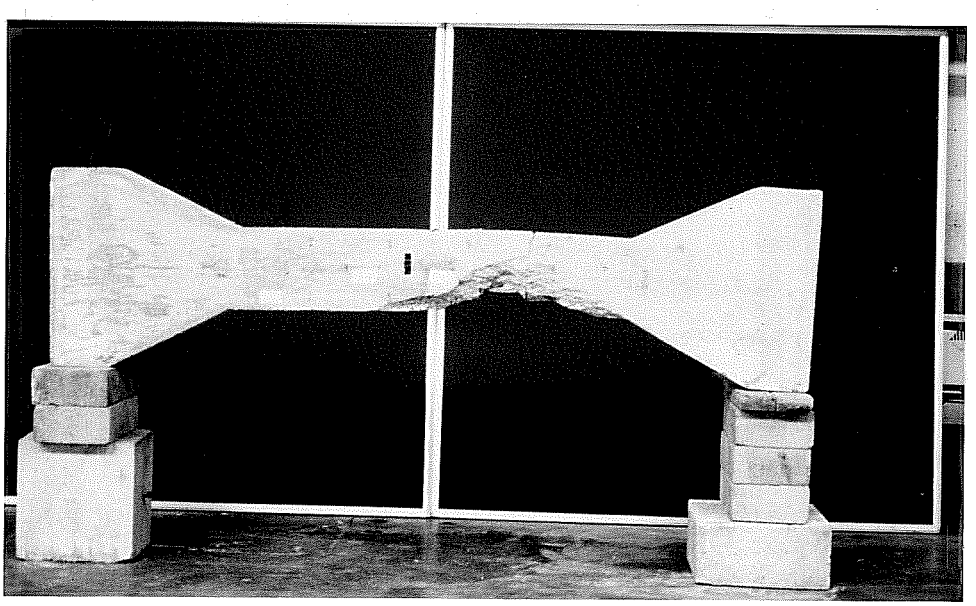

Figure 3.11 Failed normal strength concrete specimen

Table 3.2 Values of ultimate axial load, eccentricity, moment, and strain

Specimen	Axial Load (kips)	Magnified Eccen. (in.)	Moment (in-k)	Maximum Strain*10^6
CPHH1	647	0.72	465	2960
CPHH3	512	1.34	686	3260
CPHN3	509	1.34	682	3070
CPHN1	626	0.81	507	3180
CMHN1	761	0.65	495	2240
CPHH2	649	0.66	428	2120
CMHN2b	656	0.70	459	2850
CMHH1	613	0.70	429	2310*
CMHH2	654	0.69	451	2640
CPNH2	298	0.70	209	2150
CMNH1	353	0.75	265	3230
CMNH2	352	0.78	275	3150*

* indicates that a strain reading could not be taken at the final load increment

Table 3.3 Listing of the specimens that were cast out of each of the six concrete mixes

Concrete Mix Number	Specimens Cast
1	1 and 2
2	3 and 4
3	5 and 6
4	7, 8, and 9
5	10, 11, and 12
6	13, 14, and 15

Comparing the stress-strain data in Figure 3.1 with the load-strain data in Figure 3.3, it is apparent that the stiffnesses of the different concrete mixes follow a general trend relative to each other. For example, both the cylinders and the columns from mix #5 are less stiff than those from the other mixes.

The maximum strains of the high strength concrete specimens in Table 3.2 indicate that a lower or higher ultimate strain of a column corresponds with a lower or higher ultimate strain of a cylinder from the same concrete mix. This is not necessarily the case for normal strength concrete, since the maximum strain in a normal strength reinforced concrete column generally occurs beyond the strain at maximum concrete stress as obtained from a cylinder compression test.

The brittle nature of high strength concrete further adds to the variability of the limit strain of high strength concrete. Once again, it can be seen that it is desirable to use a lower limit strain for high strength concrete in order to be conservative.

CHAPTER 4
ANALYSIS AND DISCUSSION OF RESULTS

4.1 Background

Overall, the testing phase of the project was successful. The testing procedures resulted in well controlled specimen tests. Also, the measurements taken during testing were verified to be accurate. Although the number of test specimens was few, the test results can be accepted with confidence.

Based on the test results, analysis methods for predicting the limit strengths of high strength reinforced concrete columns could be evaluated, allowing for the determination of whether or not current practice is a safe and applicable approach for the design of such columns.

4.2 Overview

In the remainder of this chapter, two methods of analysis for high strength reinforced concrete columns are evaluated and discussed. The current ACI Building Code design procedure using a rectangular concrete stress block is investigated. Then, in an effort to better model the actual behavior of high strength concrete, an analysis procedure utilizing a triangular stress block is proposed. Effects of the various test variables are examined in this chapter as well.

4.3 Analysis of Specimen Behavior

4.3.1 Criteria for Evaluation of the Analysis. The main criteria for determining the appropriateness of a particular method of analysis was whether or not the calculated capacities matched the measured results of the specimen tests. In calculating specimen capacities, the axial load capacity was calculated at a given eccentricity equal to the magnified eccentricity measured at failure for a particular specimen. Therefore, a percentage difference in calculated and measured axial load would correspond with the same percentage difference in calculated and measured moment.

Another criteria regarded as being very important was that the analysis procedure should reflect the behavior of the specimen. In order to extend the principles of a particular analytical procedure to other concrete strengths, they must be representative of the material behavior.

4.3.2 Analysis Using a Rectangular Stress Block. First, capacities of the specimens were evaluated using the current rectangular stress block approach. Table 4.1 summarizes the results of this analysis.

On the average, the measured capacities of the high strength concrete specimens were about 13 percent below those calculated using the method prescribed by the ACI Building Code (ACI 318 1989). This method of analysis consistently resulted in unconservative strength predictions for the high strength concrete specimens.

As expected, results from the analysis per ACI 318 were quite close to the measured capacities for the three normal strength concrete specimens. The differences in the measured and calculated loads

Table 4.1 Comparison of calculated capacities using ACI 318 ($F_{calc.}$) with the capacities that were measured at failure ($F_{meas.}$)

Specimen	Measured Axial Load (k)	Calculated Axial Load (k)	Ratio of $F_{calc.}$ to $F_{meas.}$
CPHH1	647	712	1.10
CPHH3	512	562	1.10
CPHH2	649	816	1.26
CMHH1	613	695	1.13
CMHH2	654	728	1.11
CPHN3	509	579	1.14
CPHN1	626	709	1.13
CMHN1	761	859	1.13
CMHN2b	656	693	1.06
CPNH2	298	321	1.08
CMNH1	353	357	1.01
CMNH2	352	354	1.01

were only about 3 percent on the average. This gives added confidence to the validity of the testing program and results.

4.3.3 Basis for a Different Analysis. Since the results of the analysis per ACI 318 were unconservative by a considerable percentage, a new method of analysis was deemed necessary. This analysis should take into account the major behavioral differences between normal strength concrete and high strength concrete. These differences include the following:

1. The stress-strain relationship of high strength concrete is almost linear throughout loading as opposed to normal strength concrete which becomes significantly more nonlinear at high stresses.

2. The descending portion of the stress-strain curve is approximately vertical for high strength concrete in contrast with normal strength concrete which can sustain significantly larger strains beyond the peak stress.

3. High strength concrete is more brittle and unpredictable than normal strength concrete.

While incorporating these differences into the analysis, it is also important not to overcomplicate the necessary calculations.

4.3.4 Properties of the Proposed Stress Block. To account for the near linear stress-strain relationship of high strength concrete, a triangular stress block is proposed for concrete strengths (f'c)

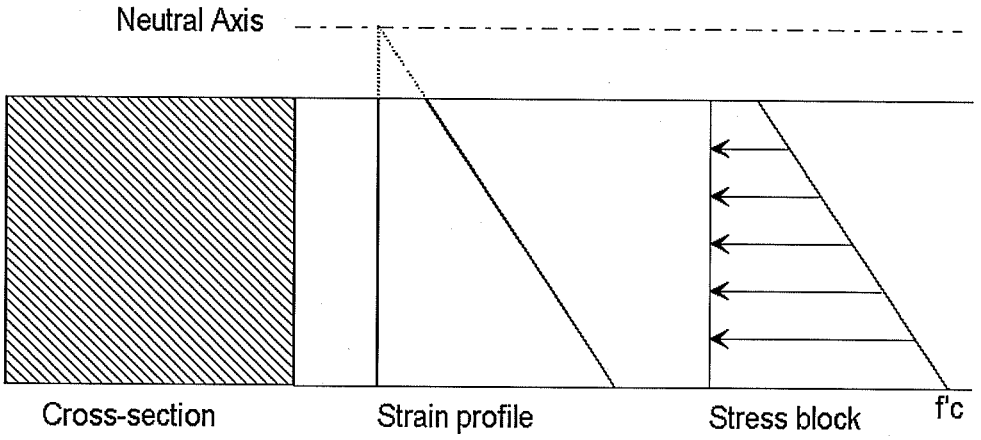

Figure 4.1 Description of the triangular stress block properties

greater than 10,000 psi. The triangular stress block has a maximum stress of f'c and decreases linearly with strain as shown in Figure 4.1. Any contribution of the concrete in tension is neglected.

Based on the results of these specimens, it is also recommended that the limit strain be reduced from 0.003 to 0.0025. Due to the linear and brittle behavior of high strength concrete, this reduction is deemed necessary so that the design method will be conservative. Although the strain at peak stress for high strength concrete may be greater than for normal strength concrete, no significant stress in high strength concrete can be sustained at higher strains. Strain beyond the peak stress can not be relied upon for high strength concrete as it can for normal strength concrete. Also, since varying the limit strain with concrete strength would not significantly improve the accuracy of the results, a single value of limit strain was chosen for a range of concrete strengths.

4.3.5 Analysis Using the Triangular Stress Block. The results of the analysis of the high strength concrete columns using the proposed triangular stress block are shown in Table 4.2. Appendix A shows a detailed example using this method of analysis.

Limit strengths predicted using the triangular stress block correlated well with the measured specimen capacities. Calculated strengths were only an average of 3 percent greater than the measured ones. If specimen 9 is omitted, the average difference is reduced to 1 or 2 percent. Considering the normally unpredictable nature of concrete, utilizing the proposed triangular concrete stress block resulted in highly accurate predictions of limit load.

Comparable results were obtained by taking the average measured strains on the top and bottom faces and assuming a linear relationship between stress and strain. The maximum stress, corresponding with the average strain on the bottom face of each specimen, was taken equal to the concrete cylinder strength (f'c). The stress on the top face was simply the ratio of the minimum to maximum strains multiplied by f'c. Stresses in the reinforcing steel were determined from the linear strain profile as well. Once again, any contribution by the concrete in tension was neglected. From these stresses, an axial load and a moment, as expressed in Table 4.3, could be calculated. Calculation procedures were similar to those in Appendix A.

Table 4.2 Comparison of calculated capacities ($F_{calc.}$) using the proposed triangular stress block with measured failure loads ($F_{meas.}$)

Specimen	Measured Axial Load (k)	Calculated Axial Load (k)	Ratio of $F_{calc.}$ to $F_{meas.}$
CPHH1	647	653	1.01
CPHH3	512	495	0.97
CPHH2	649	757	1.17
CMHH1	613	640	1.04
CMHH2	654	673	1.03
CPHN3	509	509	1.00
CPHN1	626	640	1.02
CMHN1	761	815	1.07
CMHN2b	656	649	0.99

Table 4.3 Ratios of calculated to measured axial force (P) and moment (M) where the calculated loads were determined by using a triangular stress distribution and measured strains

Specimen	Ratio of $P_{calc.}$ to $P_{meas.}$	Ratio of $M_{calc.}$ to $M_{meas.}$
CPHH1	0.97	1.11
CPHH3	0.94	1.01
CPHH2	1.10	1.23
CMHH1	0.99	1.08
CMHH2	0.98	1.13
CPHN3	0.98	1.05
CPHN1	0.94	1.21
CMHN1	1.08	0.98
CMHN2b	0.94	1.10

The results from the analysis using measured strains were similar to those obtained with the proposed triangular stress block. Based on an average, the calculated axial loads were about 1 percent below the measured values while the calculated moments were about 10 percent greater than those measured. However, considering that a 2 percent increase in moment corresponds with only about a 1 percent loss of axial load capacity, the calculated strengths again were about 3 percent over the measured capacities.

4.3.6 Discussion of Results from the Analysis. Based on the results, it is maintained that a triangular stress block with a maximum stress of f'c at a strain of 0.0025 better represents the behavior of high strength concrete columns and allows for more accurate prediction of their limit strengths. Use of the currently used rectangular stress block is unconservative as it overpredicts the strengths of reinforced columns constructed of concretes with strengths above 10,000 psi to 12,000 psi. Figure 4.2 graphically compares the results of the two analysis procedures.

4.3.7 Comparing Conclusions from the Analysis with the Literature. There is general agreement that for high strength concrete members, important differences may occur that should be addressed in eccentrically loaded columns and over-reinforced beams. Notable is the difference in compressive stress distribution of the concrete particularly at loads near ultimate (ACI Committee 363 1984). Zia and others have experimentally derived the stress block parameters for high strength concrete (Zia 1977, Perenchio 1978, Pastor 1984). Their results indicate that there are significant differences in the separate parameters depending on concrete strength.

Alternatives to the rectangular stress block have been proposed by others. Pastor and Nilson proposed a trapezoidal stress block (Pastor 1984). Leslie, Rajagopolan, and Evergard agree that a triangular stress block will better predict the behavior of high strength concrete members (Leslie 1976).

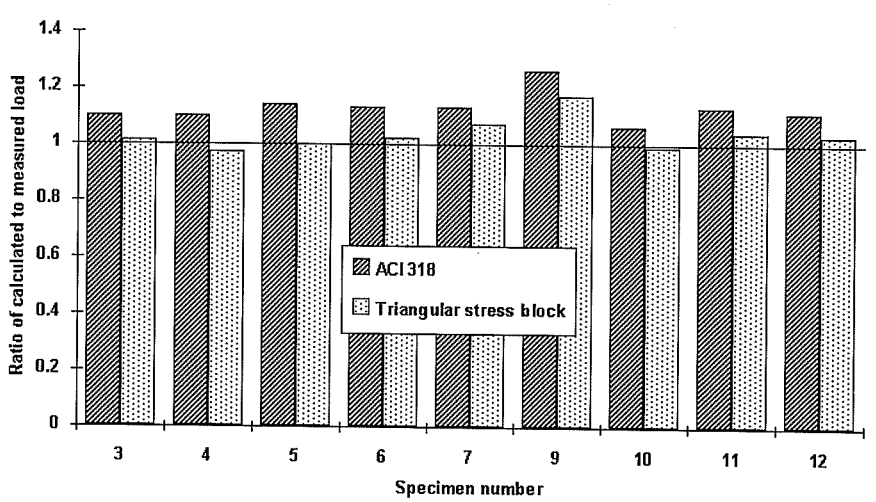

Figure 4.2 Comparison of the proposed analysis using a triangular stress block with an analysis using ACI 318

4.4 Effect of Test Variables

4.4.1 Concrete Strength. Concrete strength was not intended to be a test variable, but the high strength concrete strengths ranged from about 14,000 psi to 17,000 psi. Results seem to indicate that either analysis procedure presented in this report becomes more unconservative as the concrete strength increases. The average ratio of the calculated to measured strength of the 2 specimens with concrete strengths nearing 17,000 psi, was 1.12 using the triangular concrete stress block and 1.20 using the rectangular concrete stress block. A similar ratio for the remaining 7 high strength concrete specimens with concrete strengths around 14,000 psi was less than 1.01 using the triangular stress block and 1.11 using the rectangular stress block.

Although the amount of test data is too small to draw comprehensive conclusions regarding variable concrete strength, there is an apparent trend that might be necessary to address in an actual design procedure. The failures seem to become more brittle and unpredictable at higher concrete strengths. To account for this trend, perhaps the maximum stress of the triangular stress block should be reduced as concrete strength increases. The results of this project indicate that decreasing the maximum stress from f'c to 0.9 f'c as concrete strength (f'c) increases from 10,000 psi to 20,000 psi would be one possibility.

4.4.2 Reinforcement. The reinforcement variables including strength and arrangement of longitudinal reinforcement, and spacing of transverse steel had little or no effect on the limit strength behavior of the reinforced concrete specimens. The test results did not show evidence of any trends due to the reinforcement variables within the scope of this project. Table 4.4 shows the average calculated to measured load ratios, as determined using the triangular stress block, which indicate the effects of different variables.

Table 4.4 Effect of reinforcement variables on the average ratios of calculated ($F_{calc.}$) to measured loads ($F_{meas.}$)*

Category	Average Ratio of $F_{calc.}$ to $F_{meas.}$
High strength reinforcement	1.04
Normal strength reinforcement	1.02
Smaller tie spacing	1.06
Larger tie spacing	1.04
Model specimens	1.03
Prototype specimens	1.03

* calculated loads determined by using the proposed triangular stress block

Premature failure of the specimens with normal strength reinforcement and larger tie spacings was anticipated because of the reinforcements loss of stiffness upon yielding. In theory, this loss of stiffness coupled with a larger tie spacing could cause the concrete cover to spall off because of the

reinforcements greater tendency to buckle. However, no indications of this phenomena were apparent from the test results. Neither increasing the yield strength of longitudinal steel nor reducing the spacing of transverse reinforcement seemed to have a significant effect on the limit state behavior of the columns specimens.

Since failure strains of the specimens were low, there was little advantage in using high strength longitudinal reinforcement. The maximum steel stress as determined from exterior concrete strains was only about 75 ksi. In order to take advantage of high strength reinforcement, increased tie reinforcement for confinement needs to be provided to develop higher strains.

CHAPTER 5
CONCLUSIONS

5.1 High Strength Concrete Behavior

To model the behavior of high strength reinforced concrete columns it is necessary to have a good understanding of the stress-strain characteristics of high strength concrete. The relationship between stress and strain is more linear over a greater range for high strength concrete and can be reasonably approximated by a straight line. Also, high strength concrete is extremely brittle. No further strain capacity can be counted on beyond the strain at peak stress unless significant confinement is provided.

The modulus of elasticity of concrete depends largely on the quantity and type of coarse aggregate. Concretes containing more coarse aggregate or stiffer coarse aggregate will have higher overall stiffnesses.

Strain capacities of unconfined high strength concrete are low. Although the strain at maximum stress may be slightly higher for high strength concrete than normal strength concrete, the total strain at failure is normally less for high strength concrete.

5.2 Predicting the Limit Strength of High Strength Reinforced Concrete Columns

An appropriate analytical procedure must accurately predict limit strength. In order to accurately predict strength, the behavior of the materials must be reasonably represented. Consequently, the use of a rectangular stress block with a maximum strain of 0.003 is not valid for high strength concrete.

Because of the linear stress-strain characteristics of high strength concrete, a triangular stress block is a much better approximation of its behavior. In addition, a maximum strain of 0.0025 is more appropriate since unconfined high strength concrete cannot sustain a significant amount of strain beyond the peak stress.

Comparing test results with analysis, it is even more apparent that the use of a triangular concrete stress block results in far more accurate determinations of column strength. Employing the triangular stress block for analysis, strength predictions were normally within a few percent of the measured failure load. In contrast, using the rectangular stress block of ACI 318 consistently resulted in overestimates of strength.

Certainly, the concrete stress block as defined by ACI 318 needs to be modified to reflect the behavioral differences between normal and high strength concrete. Otherwise, design practices may be unsafe. The proposed triangular concrete stress block better reflects the behavior of high strength concrete. A design procedure incorporating a triangular concrete stress block would allow for continued safe design of reinforced concrete columns. In addition, such a design procedure would not be significantly more complicated than current design practice.

5.3 Suggestions for Further Research

Continued research regarding high strength reinforced concrete columns is essential. More test data is needed, and other variables should be investigated.

A research project involving reinforced concrete columns constructed of concretes with strengths ranging from about 8000 psi to 20,000 psi would be extremely beneficial. A study of this nature would help to determine behavioral trends in the transition region from normal strength concrete to high strength concrete.

Another valuable research study would be one in which high strength concrete is produced with varying mix designs. Important variables include both the quantity and type of coarse aggregate, and whether or not silica fume is included in the mix. The effect of these variables on the limit state behavior of high strength reinforced concrete columns may be significant.

The importance of continued research on high strength concrete cannot be emphasized enough. Design of structures with high strength concrete members has preceded the research necessary in providing sufficient knowledge of the performance of high strength concrete. This knowledge is vital in ensuring that design practices are safe.

APPENDIX A
EXAMPLE USING THE PROPOSED TRIANGULAR STRESS BLOCK

Notation

A: cross-sectional area of a single reinforcing bar.

A_{s1}, A_{s2}, A_{s3}: cross-sectional area of the corresponding layer of reinforcement where numbering is from bottom to top.

c: distance to the neutral axis.

C_1, C_2, C_3: total force in the corresponding layer of reinforcement.

C_c: total force in the concrete.

d_1,d_2,d_3: distance from the bottom of the specimen cross-section to the corresponding layer of reinforcement.

E_s: modulus of elasticity of steel (29,000 ksi).

f'_c: concrete cylinder strength.

f_y: yield strength of longitudinal reinforcement.

M: moment sustained by the reinforced concrete specimen.

P: axial load sustained by the reinforced concrete specimen.

ϵ_1, ϵ_2, ϵ_3: strain in the corresponding layer of reinforcement.

σ_{top}: concrete stress at the top of the cross-section.

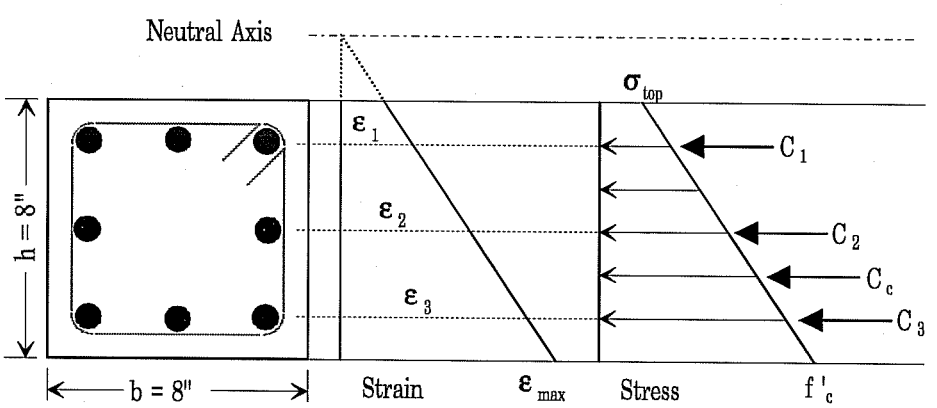

Specimen Properties

Concrete: $f'_c = 13.04$ ksi; $\epsilon_{max} = 0.0025$

Steel: #5 Diwidag bars ($A = 0.28$ in^2); $f_y = 118$ ksi; $E_s = 29{,}000$ ksi

$d_1 = 1.10$ in; $d_2 = 3.98$ in; $d_3 = 6.90$ in

$A_{s1} = 0.84$ in^2; $A_{s2} = 0.58$ in^2; $A_{s3} = 0.84$ in^2

Equations

$$\varepsilon_1 = \frac{(c-d_1)}{c}(0.0025)$$

$$\varepsilon_2 = \frac{(c-d_2)}{c}(0.0025)$$

$$\varepsilon_3 = \frac{(c-d_3)}{c}(0.0025)$$

$$C_c = f_c[\frac{h}{2}(1+\frac{(c-h)}{c})]b$$

$$P = C_1 + C_2 + C_3 + C_c$$

$$M = C_1(\frac{h}{2}-d_1) + C_2(\frac{h}{2}-d_2) + C_3(\frac{h}{2}-d_3) + \frac{(f_c - \sigma_T)}{2}(b)(\frac{h^2}{6})$$

$$C_1 = A_{s1}[\varepsilon_1(E_s) - \frac{(c-d_1)}{c}(f_c)]$$

$$C_2 = A_{s2}[\varepsilon_2(E_s) - \frac{(c-d_2)}{c}(f_c)]$$

$$C_3 = A_{s3}[\varepsilon_3(E_s) - \frac{(c-d_3)}{c}(f_c)]$$

Solving Equations

1. Estimate the neutral axis distance and solve for the axial load.
2. Iterate until the calculated axial load equals the measured axial load.
3. Calculate the moment capacity.

Solution

c = 11.8 in.

P = 640 kips

M = 449 kip-in.

BIBLIOGRAPHY

1. ACI Committee 318, *Building Code Requirements for Reinforced Concrete, ACI 318-89 and Commentary*, ACI 318R-89, American Concrete Institute, Detroit, 1989.

2. ACI Committee 363, State of the Art Report on High Strength Concrete,ACI 363R-84, American Concrete Institute, Detroit, 1984.

3. Breen, J.E., "Useful Techniques in Direct Modeling of Reinforced Concrete Structures," *Special Publication 24*, Symposium on the Use of Concrete Models for Design, American Concrete Institute, Detroit, 1970.

4. Carrasquillo, R.L., Nilson, A.H., and Slate, F.O., "Properties of High Strength Concrete Subject to Short-Term Loads, *Journal of the American Concrete Institute*, Proc. Vol. 78, No.3, May-June 1981, pp.171-178.

5. Castrodale, Reid W., Burns, Ned H., and Kreger, Michael E., "A Study of Pretensioned High Strength Concrete Bridge Girders in Composite Highway Bridges--Laboratory Tests," *Research Report 381-3*, Center for Transportation Research, The University of Texas at Austn,January 1988, pp. 9-24.

6. Cook, J.E., "10,000 psi Concrete," *Concrete International*, Vol. 10, No. 10,American Concrete Institute, Detroit, October 1989, pp. 67-75.

7. Fafitis, A. and Shah, S.P., "Predictions of Ultimate Behavior of Confined Columns Subjected to Large Deformations," *Journal of the American Concrete Institute*, Proc. Vol. 82, No. 4, July-Aug. 1985, pp. 423-432.

8. Kaar, P.H., Fiorato, A.E., Carpenter, J.E. and Corley, W.G., "Limiting Strains of Concrete Confined by Rectangular Hoops," *Research and Development Bulletin RD053.01D*, Portland Cement Association, 1978.

9. Leslie, K.E., Rajagopalan, K.S. and Evergard, N.J., "Flexural Behavior of High-Strength Concrete Beams," *Journal of the American Concrete Institute*, Proc. Vol. 52, No. 6, Sept. 1976, pp. 517-521.

10. Pastor, J.A., Nilson, A.H., and Slate, F.O., "Behavior of High Strength Concrete Beams," *Research Report No. 84-3*, Department of Structural Engineering, Cornell University, Ithaca, Feb. 1984.

11. Perenchio, William F., and Klieger, Paul, "Some Physical Properties of High Strength Concrete," *Research and Development Bulletin No. RD056.01T*, Portland Cement Association, Skokie, 1978.

12. Randall, V.R., "High Strength Concrete for Pacific First Center, "*Concrete International*, American Concrete Institute, Detroit, April 1989.

13. Zia, Paul, "Structural Design with High Strength Concrete," *Report No. PZIA-77-01*, Civil Engineering Department, North Carolina State University, Raleigh, Mar. 1977.